

## Determining the decomposition voltage of $\text{Cu}(\text{In}_{1-x}\text{Ga}_x)\text{Se}_2$

Bakker, Klaas; Matas, Joaquin Coll; Bosman, Johan; Barreau, Nicolas; Weeber, Arthur; Theelen, Mirjam

**DOI**

[10.1109/PVSC48317.2022.9938940](https://doi.org/10.1109/PVSC48317.2022.9938940)

**Publication date**

2022

**Document Version**

Final published version

**Published in**

2022 IEEE 49th Photovoltaics Specialists Conference, PVSC 2022

**Citation (APA)**

Bakker, K., Matas, J. C., Bosman, J., Barreau, N., Weeber, A., & Theelen, M. (2022). Determining the decomposition voltage of  $\text{Cu}(\text{In}_{1-x}\text{Ga}_x)\text{Se}_2$ . In *2022 IEEE 49th Photovoltaics Specialists Conference, PVSC 2022* (pp. 381-383). (Conference Record of the IEEE Photovoltaic Specialists Conference; Vol. 2022-June). IEEE. <https://doi.org/10.1109/PVSC48317.2022.9938940>

**Important note**

To cite this publication, please use the final published version (if applicable).  
Please check the document version above.

**Copyright**

Other than for strictly personal use, it is not permitted to download, forward or distribute the text or part of it, without the consent of the author(s) and/or copyright holder(s), unless the work is under an open content license such as Creative Commons.

**Takedown policy**

Please contact us and provide details if you believe this document breaches copyrights.  
We will remove access to the work immediately and investigate your claim.

***Green Open Access added to TU Delft Institutional Repository***

***'You share, we take care!' - Taverne project***

**<https://www.openaccess.nl/en/you-share-we-take-care>**

Otherwise as indicated in the copyright section: the publisher is the copyright holder of this work and the author uses the Dutch legislation to make this work public.

# Determining the decomposition voltage of $\text{Cu}(\text{In}_{1-x}\text{Ga}_x)\text{Se}_2$

Klaas Bakker<sup>1,4</sup>, Joaquin Coll Matas<sup>1</sup>, Johan Bosman<sup>1</sup>, Nicolas Barreau<sup>2</sup>, Arthur Weeber<sup>3,4</sup> and Mirjam Theelen<sup>1</sup>

<sup>1</sup>TNO - Solliance, High Tech Campus 21, 5656 AE Eindhoven, The Netherlands

<sup>2</sup>Université de Nantes, Institut des Matériaux Jean Rouxel, 2 rue de la Houssinière, BP 32229, 44322 Nantes Cedex 3 France.

<sup>3</sup>TNO Energy Transition - Solar Energy, Westerduinweg 3, 1755 LE, Petten, The Netherlands

<sup>4</sup>Delft university of Technology, PVMD, Mekelweg 4, 2628 CD Delft. The Netherlands

**Abstract**—Partial shading of CIGS modules can lead to permanent damage of the module in the shaded area. This is caused by harmful reverse bias voltages in the shaded area which lead to reverse bias induced defects, also known as wormlike defects. A lot is already known about the origin and propagation of wormlike defects. However, the fundamental question; why is CIGS so sensitive to reverse bias damage? has not yet been answered. In this study we show that CIGS semiconductor material in the presence of an electric field will spontaneously decompose.

**Keywords**—CIGS, reverse bias, decomposition, partial shading, reliability

## I. INTRODUCTION

Partial shading of CIGS modules can lead to permanent damage in the shaded area. A recent literature review [1] showed that in all studies that measured electroluminescence (EL) measurements after performing shading tests on CIGS modules permanent damage was found. In EL these defects appear as shunts. Closer visual inspection learns that the defects have a very distinct appearance and are therefore often called wormlike defects. Wormlike defects are caused by a large negative voltage (reverse bias) and are trails of damaged material left behind by a propagating hotspot. They act as local shunts that permanently decrease module performance.

Research to the origin of these defects [2], [3] showed that a chemical reaction is responsible for a change in composition, and that the reaction propagates to a new spot when the material is consumed. In a previous study [3] it was observed that the TCO conductivity influences the propagation patterns and it was concluded that the electric field has an important contribution in the formation and propagation of wormlike defects. Further evidence for the influence of the electric field was found in a study between the relation of absorber thickness and reverse bias voltage required to start wormlike defects [4]. In this study it was shown that thinner cells required a much smaller voltage to form wormlike defects.

The observed dependency on the electric field made us hypothesize that the chalcogenide CIGS structure decomposes under influence of a large electric field to the copper poor

ordered vacancy compound (OVC) and copper selenide. The reaction would be  $\text{Cu}(\text{In}_{1-x}\text{Ga}_x)\text{Se}_2$  decomposes in  $\text{Cu}(\text{In}_{1-x}\text{Ga}_x)_3\text{Se}_5 + \text{Cu}_2\text{Se}$  or  $\text{Cu}(\text{In}_{1-x}\text{Ga}_x)_5\text{Se}_8 + 2\text{Cu}_2\text{Se}$ . This hypothesis is further supported by the fact that several studies on the compositional changes in wormlike defects observed Cu rich islands in the damaged material [5], [6].

The conditions of the initial reaction that forms wormlike defects in CIGS solar cells is complicated to detect. In this study the decomposition of CIGS semiconductor material used in solar cells under the influence of an electric field is determined, using a dedicated sample configuration. With this sample configuration the conductivity of the CIGS material can be measured using a simple one dimensional approach. By varying the electric field changes in conductivity can be detected and linked to changes in the CIGS material. To the best of our knowledge this is the first time that it is shown that CIGS decomposes when a large electric field is applied. This is an important step towards understanding the complex mechanism behind the formation of wormlike defects.

## II. EXPERIMENTAL

A dedicated sample configuration was developed to measure the conductivity of CIGS semiconductor material with different compositions. Fig. 1 shows a schematic representation of the sample layout as well as a microscope picture of the molybdenum electrodes. The process steps shown in Fig. 1 (a) are:

1. Deposition and laser structuring of the 400 nm Mo layer.
2. Coevaporation of 2  $\mu\text{m}$  3-stage CIGS and sputtering of a 150 nm i-ZnO capping layer.
3. Isolating of CIGS and opening the contacts by manually removing CIGS with a scalpel. Contacting with silver paint.

The i-ZnO capping layer is added to protect the CIGS and does not play a role in the electrical characterization. The laser pattern is designed to leave a gap between rounded electrodes, that has a defined distance. Two different laser patterns were used with a gap between electrodes of 32 or 86  $\mu\text{m}$ . Electrical characterization was performed by an  $I/V$  sweep from 0 to 50 V

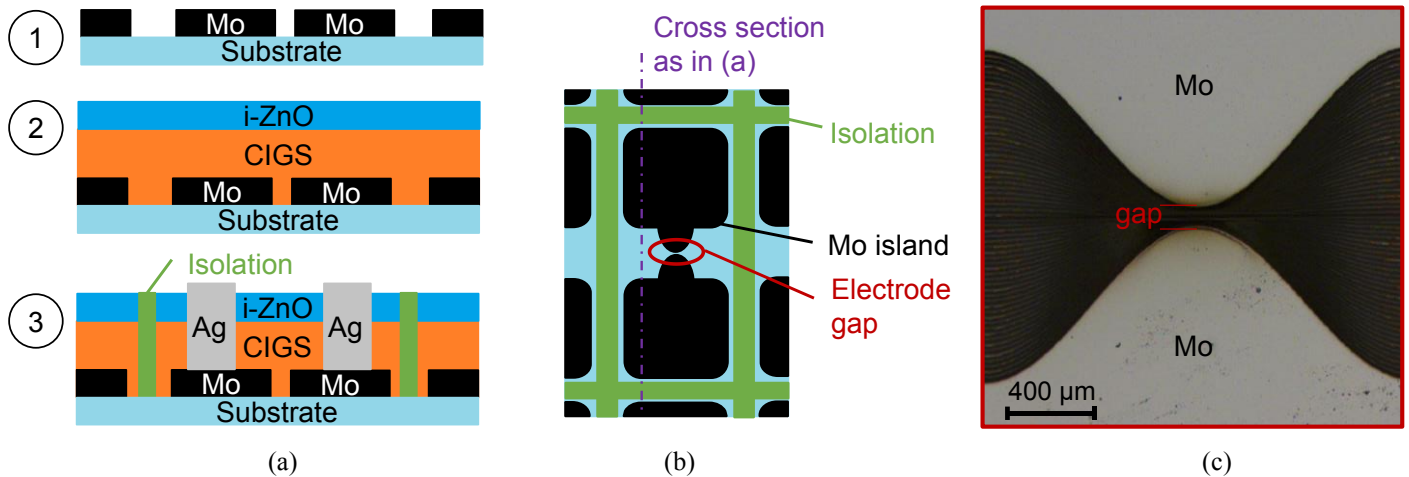


Fig. 1. Schematic and microscope photo of sample layout. In (a) a schematic cross section is given with from top to bottom the process 1 to 3 steps. A schematic top view is drawn in (b) to indicate the approximate shape of the Mo islands after step 1 and the position of the isolation scribes after step 3. (c) Shows a microscope image of the electrode gap after laser scribing (step 1).

in the dark with a Keithley 2400 source measure unit controlled by Rera tracer III software. After contacting, the sample was kept in the dark for a minimum of 60 seconds before performing the  $IV$  sweep.

### III. RESULTS AND DISCUSSION

Fig. 2 shows a typical  $IV$  curve of an electrode pair with a gap of  $86 \mu\text{m}$ . At low voltages the  $IV$  curve follows a straight line, showing Ohmic behavior. At higher voltages the behavior deviates from the straight line, followed by a sharp change in current. This change in current could be both positive or negative and indicates a change in material properties. Therefore, we propose the term *decomposition voltage* for this point on the  $IV$  curve, because after this point visual compositional changes appear similar to wormlike defects.

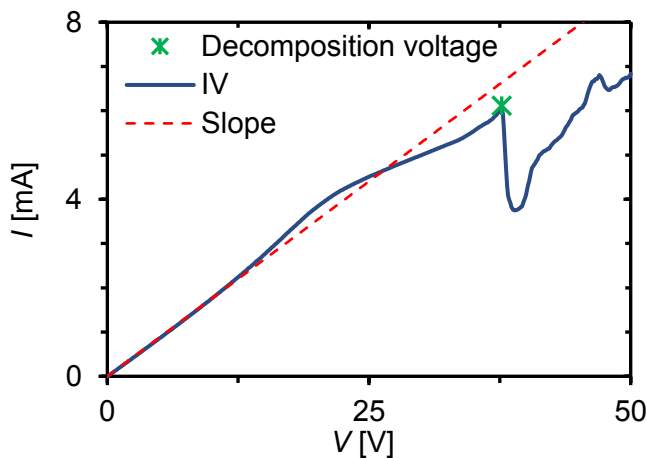


Fig. 2.  $IV$  curve of sample with a  $86 \mu\text{m}$  electrode gap. The measured  $IV$  curve is plotted as a blue solid line. The red dotted line is a superpolation of the average slope between 0 and 10 V to indicate ohmic behavior. The decomposition voltage is indicated with a green asterisk

The sharp change in current observed during the  $IV$  sweeps is very similar to the increase in current during the formation of wormlike defects [4]. The visual appearance after decomposition is also very similar to the visual appearance of

wormlike defects. A microscope picture of a sample after an  $IV$  sweep can be found in Fig. 3. The composition of the defects has not been studied in detail yet. However, initial microscopy and Raman measurements showed similarities with wormlike defects, created by reverse bias in CIGS solar cells. Just like in studies of wormlike defects no traces of OVC or  $\text{Cu}_2\text{Se}$  have been found. The reaction is so aggressive that it is likely that the initial reaction products (OVC +  $\text{Cu}_2\text{Se}$ ) are consumed in a sequential reaction that gives the wormlike defects its distinct appearance.

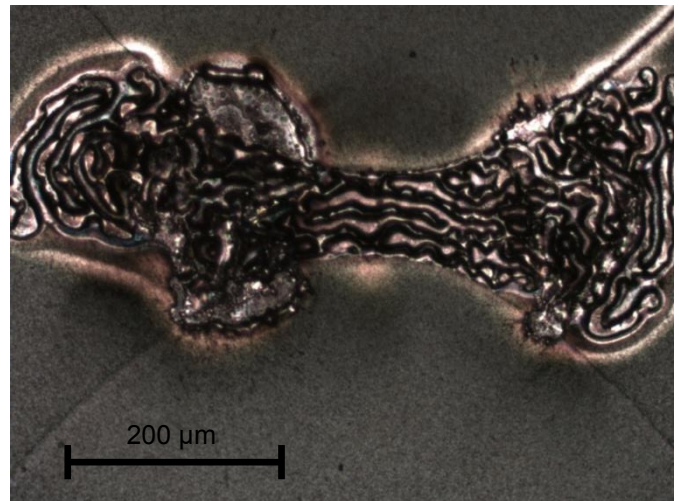


Fig. 3. Microscope picture of decomposed CIGS between two electrodes with a gap of  $86 \mu\text{m}$ .

Because of the 1D approach the measurements are very reproducible. A large number of samples with CGI (copper/(gallium + indium)) varying from 0.795 to 0.894 was examined. All measurements showed the same behavior, as can be seen in Fig. 4 where all measurements with a  $32 \mu\text{m}$  electrode gap are plotted up to the decomposition voltage. The different shades of blue represent the copper content.

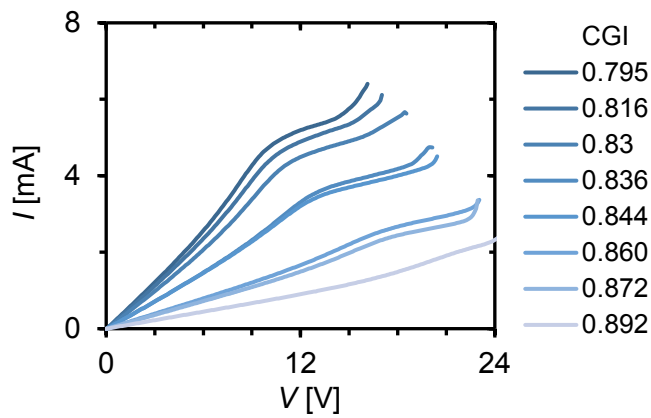


Fig. 4. IV curves of all samples with a 32  $\mu\text{m}$  electrode gap up to the decomposition voltage. The CGI of each sample is plotted in different shades of blue, with the darkest color being the lowest CGI.

From Fig. 4 it can be seen that both slope and decomposition voltage depend on the CGI. Therefore, the dependency of the normalized resistance and normalized decomposition voltage on the CGI is given in Fig. 5. The normalized resistance has a logarithmic dependency on CGI. The normalized decomposition voltage, or electric field, is depending linearly on the CGI, with the larger gap being less sensitive to the difference in copper concentration. This might be a geometric effect caused by the shape of the electrodes.

The exact relationships are still unclear. However, the conductivity is depending on carrier density and mobility so it is not unlikely that the semiconductor parameters have a large influence on the decomposition properties.

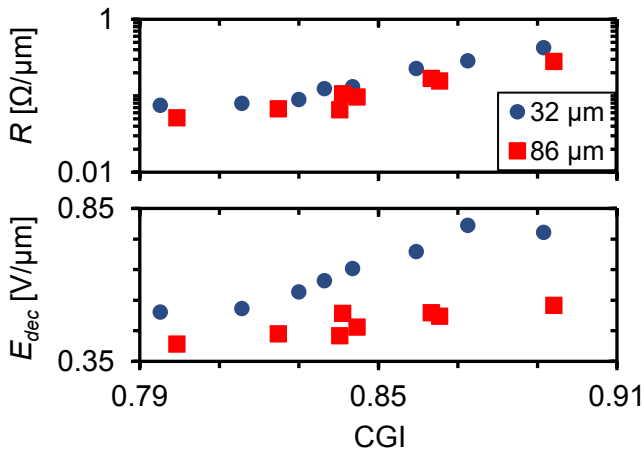


Fig. 5. Resistance and decomposition voltage normalized to electrode distance plotted against CGI for two different electrode gaps. In all graphs the 32 and 86  $\mu\text{m}$  gaps are represented by dark blue circles and red squares, respectively.

#### IV. SUMMARY

The formation of wormlike defects during reverse bias is a major reliability concern for CIGS solar cells and modules. One of the unknown parameters required to predict the formation and propagation of wormlike defects is the sensitivity of CIGS towards an electric field. This is difficult to determine in the traditional rather complicated CIGS solar cell stack. Therefore, a dedicated device structure was developed to measure the

influence of an electric field on the CIGS absorber material used in solar cell. IV measurements on these structures showed that CIGS material is spontaneously decomposing. We proposed the term decomposition voltage for the electrical voltage required for decomposition. The decomposition voltage was found to be depending on CGI. The approach used in this study changed the puzzle of decomposition of CIGS from the complicated solar cell stack to a simple one-dimensional approach and proved that CIGS is unstable in the presence of a large electric field. Therefore, CIGS solar cells need to be protected against the harmful effects of reverse bias.

#### REFERENCES

- [1] K. Bakker, A. Weeber, and M. Theelen, "Reliability implications of partial shading on CIGS photovoltaic devices: A literature review," *J. Mater. Res.*, vol. 34, no. 24, pp. 3977–3987, Dec. 2019.
- [2] K. Bakker, H. Nilsson Ahman, K. Aantjes, N. Barreau, A. Weeber, and M. Theelen, "Material Property Changes in Defects Caused by Reverse Bias Exposure of CIGS Solar Cells," *IEEE J. Photovoltaics*, vol. 9, no. 6, pp. 1868–1872, Nov. 2019.
- [3] K. Bakker, H. N. Åhman, T. Burgers, N. Barreau, A. Weeber, and M. Theelen, "Propagation mechanism of reverse bias induced defects in  $\text{Cu}(\text{In,Ga})\text{Se}_2$  solar cells," *Sol. Energy Mater. Sol. Cells*, vol. 205, p. 110249, Feb. 2020.
- [4] K. Bakker, A. Rasia, S. Assen, B. Ben Said Aflouat, A. Weeber, and M. Theelen, "How the absorber thickness influences the formation of reverse bias induced defects in CIGS solar cells," *EPJ Photovoltaics*, vol. 11, no. 9, Nov. 2020.
- [5] P. O. Westin, U. Zimmermann, L. Stolt, and M. Edoff, "Reverse Bias Damage in CIGS Modules," in *24th European Photovoltaic Solar Energy Conference*, 2009, pp. 2967–2970.
- [6] H. Guthrey *et al.*, "Characterization and modeling of reverse-bias breakdown in  $\text{Cu}(\text{In,Ga})\text{Se}_2$  photovoltaic devices," *Prog. Photovoltaics Res. Appl.*, vol. 27, no. 9, pp. 812–823, Sep. 2019.